AN ANALYTICAL PICTURE OF NEURON OSCILLATIONS

Paul E. Phillipson*,[a] and Peter Schuster[b]

[a] Austrian Academy of Sciences, Dr.Ignaz Seipel-Platz 2, A-1010 Wien, Austria

[b] Institut für Theoretische Chemie und Molekulare Strukturbiologie,
Universität Wien, Währingerstraße 17, A-1090 Wien, Austria and
Santa Fe Institute, Santa Fe, NM 87501, USA

* Permanent address: Department of Physics, Box 390, University of Colorado,
Boulder, CO 80309, USA

ABSTRACT

Current induced oscillations of a space clamped neuron action potential demonstrates a bifurcation scenario originally encapsulated by the four dimensional Hodgkin-Huxley equations. These oscillations were subsequently described by the two dimensional FitzHugh-Nagumo Equations in close agreement with the Hodgkin-Huxley theory. It is shown that the FitzHugh-Nagumo equations can to close approximation be reduced to a generalized van der Pol oscillator externally driven by the current. The current functions as an external constant force driving the action potential. As a consequence approximate analytic expressions are derived which predict the bifurcation scenario, the amplitudes of the oscillations and the oscillation periods in terms of the current and the physiological constants of the FitzHugh-Nagumo model. A second reduction permits explicit analytic solution and results in a spiking model which can be multiply coupled and extended to include the dynamics of phase locking, entrainment and chaos characteristic of time-dependent synaptic inputs.

Keywords: FitzHugh-Nagumo equation, Hopf bifurcation, nerve dynamics, refractory behavior, relaxation oscillation

To appear in *Internat. J. Bifurcation and Chaos*, **14**, May 2004 issue.

Mailing address: Paul Phillipson, Department of Physics, Box 390
University of Colorado at Boulder
Boulder, CO 80309, U.S.A.
E-Mail: phillipe@colorado.edu
Fax: (303) 492 3352
Tel. (303) 492 6942

1 Introduction

Investigations of the electrochemistry of a neural pulse initiated by Helmholtz in the nineteenth century [Scott, 1975] reached a plateau fifty years ago when Hodgkin and Huxeley [1952] reported their detailed quantitative studies of pulse conduction and oscillation. Their results were encapsulated by a system of four coupled nonlinear differential equations [H-H model] which predict the features of the neural pulse action potential in agreement with their experiments. The full implications of the H-H model revealed by mathematical solution presented challenges not only to its authors but also to later researchers [Cole et al., 1955; FitzHugh & Antosiewicz, 1959; Cooley & Dodge, Jr., 1966] which continues to the present [Mascagni & Sherman, 1998]. The complexity of the H-H equations prompted FitzHugh [1961] to introduce a formal reduction to a more tractable two dimensional system which can be expressed in the form

$$\begin{aligned} \frac{dV}{dt} &= -V(V-a)(V-1) \, - \, Y \, + \, F \\ \frac{dY}{dt} &= bV \, - \, \epsilon Y \ , \end{aligned} \tag{1}$$

where V is the action potential, Y is a recovery variable which measures the state of excitability of the cell, and I is the current which remains to be specified. The quantities a, b, ϵ are constants related to the physiological state of the neuron. Under conditions the axon is space clamped such that the I is constant FitzHugh demonstrated these equations predict the resting, refractory and oscillatory phenomena in close identification to those demonstrated by experiment and by the H-H equations. Similar to the procedure of Hodgkin and Huxley, who extended their equations to account for neural pulse conduction along the axon, Nagumo *et.al* [1962] subsequently identified I with the second spatial derivative of the action potential to provide a mechanism for propagation. The FitzHugh-Nagumo [F-N equations] Eqs. (1) for constant I provided the first example of two dimensional dynamical models which have been developed to account for more subtle details of neural excitations and other phenomena such as bursting [Izhikevich, 2000]. Analytical connections between the two dimensional models and their extraction from H-H dynamics are to be found in a recent monograph [Gerstner & Kistler, 2002]. The purpose of the present study is to return to the F-N equations above for the space clamped case to introduce approximations designed to supplement the picture of neuron dynamics. A second goal is to provide approximate analytic relations which predict the oscillation amplitudes and periods in terms of the constants and the current. While these equations have achieved textbook status [Jackson, 1991], as will be discussed in the final section of this study, analytic simplification of these equations results in a simple, analytic spiking model which can be simply extended to treat the dynamics of more

general synaptic inputs.

2 Reductions of the FitzHugh-Nagumo Equations

Our procedure is scale the time variable according to $\tau = \sqrt{b}\,t$ and express the two first order differential equations of Eq. (2) as a single second order differential equation. Differentiation of the first equation of Eq. (2) with substitution of the second equation leads to the F-N model in a form which will be simply approximated by two successive reductions denoted by arrows according to

$$\frac{d^2V}{d\tau^2} = -k(V-q_1)(V-q_2)\frac{dV}{d\tau} + \Big[I' - V\Big] - \frac{\epsilon}{b}\Big[V(V-a)(V-1)\Big]$$
$$\text{with } q_{1,2} \equiv \frac{1}{3}\Big[(a+1) \mp \sqrt{(a+1)^2 - 3(a+\epsilon)}\Big],\ \ k \equiv \frac{3}{\sqrt{b}},\ \ I' \equiv \frac{\epsilon}{b}I \qquad (2)$$

$$\text{FitzHugh} - \text{Nagumo Equation}$$

$$\longrightarrow \qquad \frac{d^2V}{d\tau^2} = -k(V-q_1)(V-q_2)\frac{dV}{d\tau} + I' - V \qquad (3)$$

$$\text{Reduced Model}$$

$$\longrightarrow \qquad \frac{d^2V}{d\tau^2} + \sigma k'\frac{dV}{d\tau} + V = I' \ \text{ with } \ \Big[k' = kf(V_{\min}) = \frac{k}{4}(q_1-q_2)^2\Big]$$
$$\text{and } \Big[\sigma = -1 \ \text{ for } \ q_1 < V < q_2,\ \ \sigma = +1 \ \text{ otherwise}\Big] \qquad (4)$$

$$\text{Reduced Broken} - \text{Linear Model}$$

The exact equations [2] have constants grouped into $q_{1,2}$ which will function as dynamical barriers and as quantifiers of bifurcation. The constant current I is scaled by the factor $\frac{\epsilon}{b}$, and the quantity k in terms of b alone functions as a stiffness constant parameterizing relaxation oscillation. The dynamics of the F-N equations [2] with increasing current follows a bifurcation scenario analyzed by Troy [1976]. Troy's scenario is summarized here in terms of the present construction to provide the point of departure for the subsequent simplifications of Eqs. [3,4]. The F-N equation obeys Class II dynamics [Izhikevich, 2000] characterized by Hopf bifurcation from stationarity to oscillation. There are three fixed points $V_0(I)$ determined by the current when the two terms in brackets of Eq. (2) balance, only one of which is real for the parameter and current range of neuron interest. The eigenvalues for the linearized solutions about this fixed point are $p_\pm = \lambda \pm i\omega$, where $\lambda = \frac{k(q_2-V_0)(V_0-q_1)}{2}, \omega = \frac{\sqrt{4-[k(V_0-q_1)(V_0-q_2)]}}{2}$. These eigenvalues have a positive real part provided $q_1 < V_0(I) < q_2$. Within this range the linear solutions are unstable, and in particular subcritical bifurcation to oscillation from below and above occur at $V_0 = q_1$ and $V_0 = q_2$ respectively to initially an unstable focus. Combining this result with the

fixed point condition implies that oscillations occur within the current range $I_1 < I < I_2$ where $I_{1,2} = \frac{b}{\epsilon} q_{1,2} + q_{1,2}(q_{1,2} - a)(q_{1,2} - 1)$. At $I = I_1$ the focus becomes unstable and subthreshold low amplitude oscillations centered around the lower boundary q_1 are born. These oscillations become unstable at a small intensity increment above I_1 and are succeeded by large amplitude unsymmetrical relaxation oscillation of large, spiked, maximum and a relatively shallow minimum with respect to q_1: the major fraction of the pulse duration is from the minimum to q_1. As the current progresses the oscillations become more symmetric and the period tends to decrease. The period minimum and oscillation symmetry is reached at $I_{\min} = \frac{I_1 + I_2}{2}$. Beyond this point as the current increases from $I_{\min}$ the process reverses and the oscillations again progress towards increasing asymmetry where now most of the duration of the pulse is during the time the voltage is greater than the upper boundary q_2. As I_2 is approached there is collapse back to low amplitude oscillation terminating with damped oscillatory decay at I_2. Beyond I_2 the neuron is frozen by the current into the steady state value of $V_{\rm ss} = I > I_2$.

3 Reduced Model [Equation (3)]

The F-N scenario is preserved in all details even if the cubic term $V(V - a)(V - 1)$ of the second bracket in Eq. (3) is neglected to result in the reduced model of Eq. (3). There is now the single fixed point which is just the scaled current $V_0 = I'$ and the current range for oscillation to be $I_1 = \frac{b}{\epsilon} q_1 < I < \frac{b}{\epsilon} q_2$ $[q_1 < I' < q_2]$, a slight quantitative expansion of this range compared to the F-N equation. Figures 1A and 1B show solutions of Eq. (3) to graphically demonstrate this scenario. These illustrations use the values introduced by Rinzel [1981]: $a = 0.25$ and $\epsilon = b = 0.002$. From the definition of Eq. (2) the figures are for the specific example of $I_1 = q_1 = 0.11732$, $I_2 = q_2 = 0.71602$, compared to $I_1 = 0.13106$, $I_2 = 0.62126$ for the F-N Eq. (2). The choice $\epsilon = b$ implies Hopf bifurcation occurs at these barrier points $q_{1,2}$. The pulses have the same shape and display the same dynamics as solution of the F-N Eq. (2) and reproduce closely in this regard solution of the H-H equations [Cooley & Dodge, Jr., 1966; Gerstner & Kistler, 2002]. The validity of this reduction hinges on the fact that a plot of the neglected cubic function in the range $q_1 < V < q_2$ shows it to be very small compared to the remaining terms of the F-N equation for the physiologically meaningful range of parameters. Because $b = 0.002$ is small, the stiffness constant parameterizing the F-N Eq. (2) is large, $[k = 67.08]$ which fulfills the criterion for relaxation oscillation. More generally, if $\epsilon = 0$ and $q_{1,2} = \mp 1$ the F-N equation reduces to the van der Pol equation [Jackson, 1991] which was the point of departure in FitzHugh's study. As a consequence the reduction of Eq. (3) provides a simple picture in the spirit of FitzHugh's original development: nerve impulse oscillation mod-

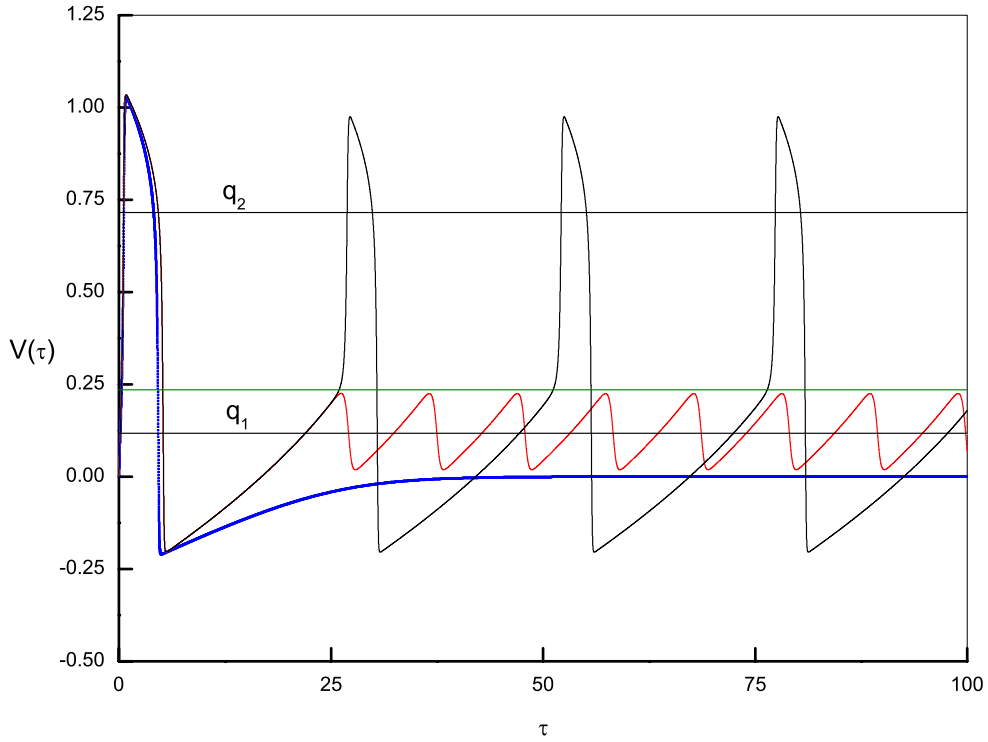
1.25
1.00
0.75
0.50
0.25
0.00
-0.25
-0.50
V(τ)
q2
q1
0
25
50
75
100
τ

A

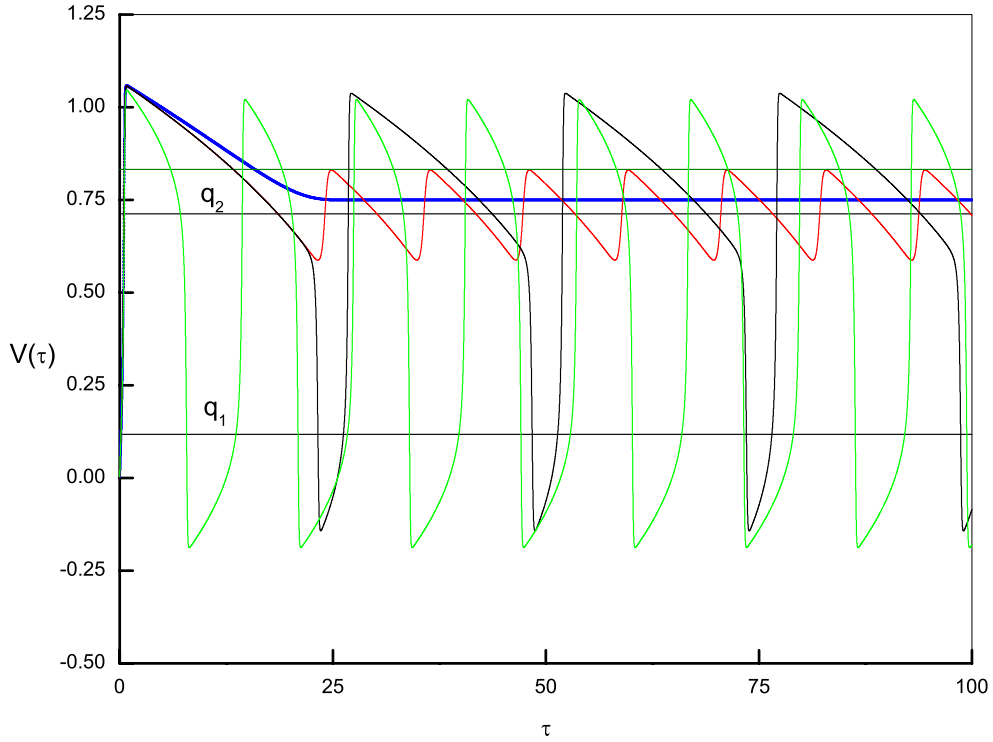
1.25
1.00
0.75
0.50
0.25
0.00
-0.25
-0.50
V(τ)
q2
q1
0
25
50
75
100
τ

B

Fig. 1. **Reduced Model, Eq. (3). Upper part, A:** Individual curves (a) Refractory behavior at I=0, (blue curve). (b) Low Amplitude oscillation at $I = 0.11837$ (red curve), (c) Large amplitude relaxation oscillation at $I = 0.11838$ (black curve). Black horizontal lines locate the dynamical boundaries at $q_1 = 0.11732,\ q_2 = 0.71602$ from Eq. (2) using the constants of Rinzel [1981]. The dark green horizontal line at $q_1 + I = 0.23569$ illustrates that the maximum of the low amplitude oscillation is almost equal to this value just prior to bifurcation to relaxation oscillation. For all figures, the initial conditions are $V(0) = 0,\ \frac{dV}{d\tau}|_0 = 1$. **Lower part, B**: Individual curves (a) Symmetric relaxation oscillation where period is a minimum: $I = \frac{q_1+q_2}{2} = 0.4167$ (green curve). (b) Oscillation at high current just prior to reverse bifurcation to small oscillation at $I = 0.71495$ (black curve). (c) collapse to small amplitude at $I = 0.71496$ (red curve) . The dark green horizontal line at $q_1 + I = 0.83228$ illustrates that the maximum of the low amplitude oscillation is equal to this value upon collapse of the relaxation oscillation (b). (d) Steady state saturation at high current (nerve block): $I = 0.75 > q_2$ (blue curve). The black horizontal lines locate the boundaries as in **A**.

eled by Eq. (3) is interpreted as produced by the scaled current I' functioning as a constant external force. The force I' drives the action potential structured as a generalized van der Pol oscillator parameterized by positive dynamical boundaries $0 < q_1 < q_2$. In particular, at zero current, linearization of Eq. (3) around zero produces eigenvalues $\lambda_{1,2} = \frac{-kq_1q_2 \pm \sqrt{(kq_1q_2)^2-4}}{2}$. Since $q_{1,2}$ are positive, regression to the resting state at zero current exemplified by the blue curve in Fig. 1A occurs because both eigenvalues are negative. This is distinct from the van der Pol equation for which $q_{1,2} = \mp 1$ resulting in positive eigenvalue and consequent limit cycle behavior. This reinforces that transition from the van der Pol equation to the F-N model, which features refractory behavior, implies necessarily the introduction of positive dynamical boundaries.

This reduction to van der Pol dynamics allows analytic determination of the transitions from small oscillation to relaxation oscillation (from the red curve to the black curve in Fig. 1A and the reverse process at high current in Fig. 1B). Relative to the fixed point at $V_0 = I'$, with $x = V - I'$ and $v = \frac{dx}{d\tau}$ indicating an analogy to 'position' and 'velocity', the reduced model Eq. (3) becomes

$$\frac{dv}{d\tau} + k\Big[x + (I' - q_1)\Big]\Big[x - (q_2 - I')\Big]v + x = 0\ .$$

The red curve oscillations are not harmonic but they are relatively small. As an approximation we assume a harmonic solution of the form $x = A\cos\phi$, $v = A\sin\phi$ and invoke the averaging procedure of Krylov & Bogoliubov[1947; Jackson, 1991] appropriate for oscillations with small departure from harmonic. Substitution into this expression and averaging over ϕ gives the result that $\frac{dA}{d\tau} = \frac{kA}{2}\left[(I' - q_1)(q_2 - I') - \frac{A^2}{4}\right] \to 0$ as $\tau \to \infty$. The dark green lines at $V = q_1 + I'$ of the red curves fall almost at the maxima of these curves just

prior to bifurcation. Approximately, therefore, transition from small to relaxation oscillation at low current (Fig. 1A) or the reverse transition at high current (Fig. 1B) occurs at current I^*, such that $A = q_1 = 2\sqrt{(I^* - q_1)(q_2 - I^*)}$. Therefore, the transition currents are

$$I^*_{\pm} = \frac{(q_1 + q_2) \pm \sqrt{q_2(q_2 - 2q_1)}}{2} \ . \tag{5}$$

For the present example this result predicts transition from low to relaxation oscillation to occur at $I^*_- = 0.123$ [0.118] and the reverse to occur at $I^*_+ = 0.710$ [0.715] where the values in brackets are the computer solution values shown in Figs. 1A and 1B – predictive agreement within 4%. This analytical result, however, is parameter-specific in that transition to or from relaxation oscillation implies a large stiffness parameter k of Eq. (2). To demonstrate refractability of his model, FitzHugh [1961] chose parameters [$a = 0.130,\ b = 0.08754,\ \epsilon = 0.0789$] which implies a stiffness parameter approximately one-sixth the present value. As a consequence the relatively soft oscillations produced by this parameter choice do not indicate sharp transition. The present choice, proposed by Rinzel, is consistent with the scenario of the action potential evolving to a sharp pulse, or spike, which is predicted by Eq. (5) in the asymptotic limit that b is very small [$k \to \infty$]. Additionally, perusal of the pulses shown in the figures indicates that the pulse amplitudes maxima and minima are almost independent of the current in the relaxation oscillation regime. This behavior can be understood by assuming that the amplitude factors A above appropriate to $V_{\max,\min}$ are given by $A_{\max,\min} = \pm 2\sqrt{(I' - q_1)(q_2 - I')}$. Since the amplitude is asymptotically insensitive to the current, we will choose the center value of $I' = \frac{\epsilon(I_1+I_2)}{2b} = \frac{q_1+q_2}{2}$ so that $A_{\max,\min} = \pm(q_2 - q_1)$ with respect to the fixed point I'. Then $V_{\max,\min} = I' + A_{\max,\min}$ so that the pulse extrema are predicted to be approximately independent of the current and determined by the control parameters defining the barriers according to

$$V_{\max} = \frac{3q_2 - q_1}{2},\ \ V_{\min} = \frac{3q_1 - q_2}{2} \ . \tag{5'}$$

In the approximation that the time spent within the $q_1 - q_2$ range is neglected, and assuming the dynamics is sufficiently slow that one puts the second derivative in the Reduced Model of Eq. (3) equal to zero, then the period of a pulse is given approximately by $T = \int \frac{dx}{v(x)}$ where the limits of integration extend [$q_2 - I'$ to $V_{\max} - I'$] and [$q_1 - I'$ to $V_{\min} - I'$]. The result is

$$\begin{aligned} T \ = & k\Bigg\{ \frac{3(q_1 - q_2)^2}{4} - \\ & - \Big[(I' - q_1)(q_2 - I')\Big] \ln\left[\frac{\Big[(3q_2 - q_1) - 2I'\Big]\Big[2I' - (3q_1 - q_2)\Big]}{4(q_2 - I')(I' - q_1)} \right] \Bigg\} \end{aligned} \tag{5"}$$

where the current range is restricted by Eq. (5"): $I_-^* < I < I_+^*$. For the symmetric case, $I' = \frac{q_1+q_2}{2}$ this expression reduces to $T = (3-2\ln 2)k', \;\; k' = \frac{k(q_1-q_2)^2}{4}$, which is asymptotically the period of a van der Pol oscillator [Jackson, 1991], linearly proportional to the stiffness constant k'. k must be sufficiently large that one can neglect corrections in reciprocal powers of k'. In this particular numerical case, $k' = 6.011$, is sufficiently small that the computed period would require this correction. For the symmetric case, the period according to the asymptotic Eq. (5") is 9.75, which is corrected to 13.56 including the $\frac{7.0143}{(k')^{\frac{1}{3}}}$ term [Dorodnitsyn, 1947; Phillipson & Schuster, 2001], in good agreement with the computer value of 13.08. Equation (5') predicts $[V_{\max}, V_{\min}] = [1.02, -0.18]$ in close agreement with the computer solution of $[1.02 \pm 0.05, -0.19 \pm 0.04]$. These asymptotic current independent expressions neglect the slight increase of $V_{\max}$ and slight decrease of $V_{\min}$ with increasing current. As b is smaller the asymptotic expressions are more accurate. For example, for $\epsilon = b = 0.0001, \;\; [k = 300, \;\; k' = 27.07]$, Eqs. (5') and (5") agree with computer solution of Eq. (3) within 4% over the total current range $I_\pm$ of Eq. (5).

4 Reduced Broken-Linear Model [Equation (4)]

The generic feature of clamped neuron dynamics is spiking. The present dynamics of achieving this through Class II Hopf bifurcation scenario is alternative to Class I dynamics where spike evolution is through saddle-node bifurcation which can be canonically modeled on an invariant circle [Izhikevich, 2000]. The most famous neuronal model which has the flexibility to display either Class I or Class II dynamics is that of Morris & Lecar [1981; Rinzel & Ermentrout, 1998]. It has been noted that, on the one hand, these two dynamical mechanisms are consistent with a myriad of ionic mechanisms, and on the other hand, that this classification is not unambiguous [Izhikevich, 2000]. These complexities are bypassed in the construction of spiking neuron models in their simplest form (such as the Integrate and Fire model) for studies of collective neural behavior associated with neural coding, memory and network dynamics [Gerstner & Kistler, 2002]. To construct a bridge between a specific bifurcation model and a simpler one which emphasizes the generic refractory and spike features of neural behavior inherent to collective neural models we replace the smooth parabolic function multiplying the first derivative in Eq. (3) by a discontinuous weighted step function to produce the Reduced Broken-Linear Model of Eq. (4). The weighting factor $f(V_{\min})$ multiplying the step $\sigma = \pm 1$ centers the dynamics such that this constant passes through the parabola minimum at $\frac{q_1+q_2}{2}$. The weighted stiffness constant k' is precisely that characterizing symmetric oscillation of the Reduced Model. This second reduction reflects the fact that the oscillations characteristic of

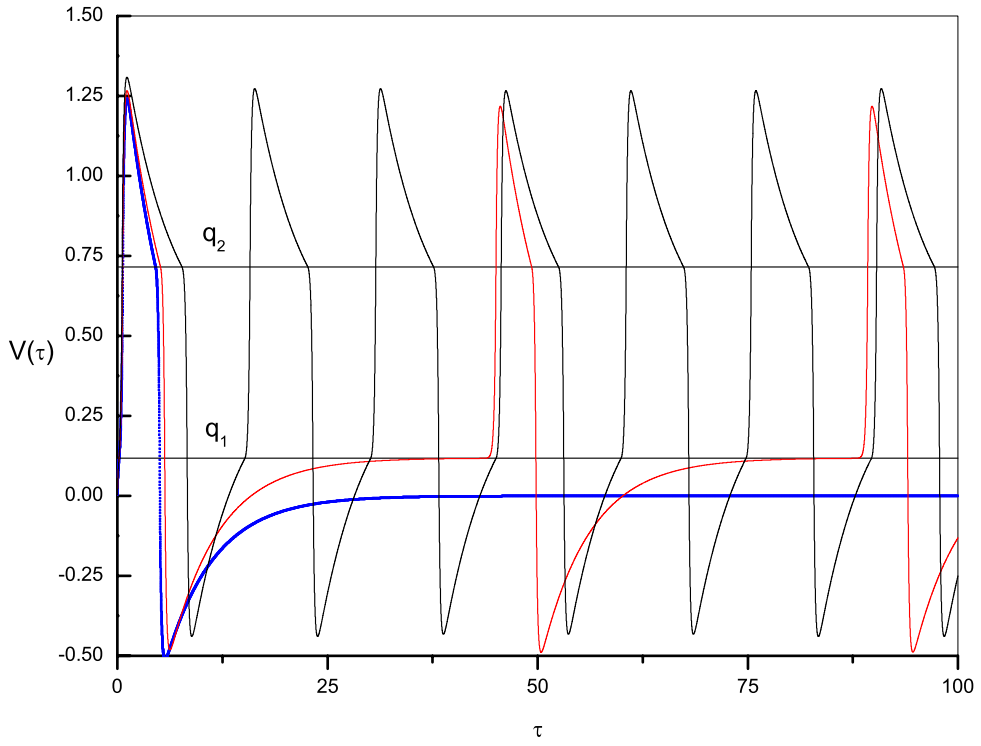

Fig. 2. **Reduced Broken-Linear Model, Eq. (4).** Individual curves: (a) Refractory behavior at I=0 (blue curve) which mimics the blue curve of the Reduced Model in Fig. 1A, (b) I=0.11837 (red curve) to be compared with the low amplitude oscillation (red curve) of the Reduced Model in Fig. 1A at the same current value. The relaxation oscillation here illustrates the all-or-nothing nature of the present model, (c) symmetric relaxation oscillation (black curve) where the period is a minimum $I = \frac{q_1+q_2}{0}.4167$ to be compared to the symmetric oscillation of the Reduced Model in Fig. 1B (gray curve). Between the two barriers the oscillations of the two models are similar except for details in the shape. These figure computed using Rinzel's choice of parameters discussed in the text, so that $k' = 6.011$ from it's definition in Eq. (4).

the F-N model feature, for b sufficiently small, large change in the pulse form in the vicinity of the $q_{1,2}$ boundaries as illustrated in Figs. 1A and 1B. The boundaries are, as a consequence of this second reduction, hard, and the resulting equations linear in the two regions separated by the boundaries and therefore exactly solvable. A different broken linear approach has been investigated by Rinzel [1978] who approximated the cubic function in the original first order F-N Eqs. (1) by a saw-tooth piecewise linear function with three linear components. This implies discontinuities in passage to a second order equation so that, as emphasized in his study, the bifurcation description required nonstandard considerations. Replacing here a quadratic term by a two piece step after passage to the second order differential equation removes this complication. Figure 2 illustrates the dynamics for representative values of the current. The blue curve at zero current again demonstrates refractability. The red curve, to be compared to the red curve of Fig. 1A illustrates the

all-or-nothing feature of the model: small amplitude oscillations are no longer present so that pulses of almost fixed amplitude evolve from sharp bifurcation at the lower boundary $I' = q_1$. With increasing current one obtains the same scenario of decreasing period to a period minimum (black curve) when the current is centered between the boundaries with the trend reversing until the upper boundary bifurcation point is reached at $I' = q_2$.

Analytical predictions of the model follow from the solution of Eq. 4. With respect to the fixed point I', $V(\tau) = I' + x(\tau)$, this solution is given by

$$x(\tau) = \frac{v(0) - s_2(\sigma)x(0)}{s_1(\sigma) - s_2(\sigma)} \exp(s_1(\sigma)\tau) + \frac{s_1(\sigma)x(0) - v(0)}{s_1(\sigma) - s_2(\sigma)} \exp(s_2(\sigma)\tau) \qquad (6)$$

$$s_1(-1) = p_1, s_2(-1) = p_2 \;\; [q_1 < V < q_2], \quad s_1(1) = -p_2, s_2(1) = -p_1 \;\; [\text{otherwise}]$$

$$p_1 = \frac{1}{2}[k' + \sqrt{(k')^2 - 4}], \;\; p_2 = \frac{1}{2}[k' - \sqrt{(k')^2 - 4}], \;\; \text{with} \;\; p_1 + p_2 = k', \;\; p_1 p_2 = 1 \; .$$

where $v(0) \equiv \frac{dV}{d\tau}\Big|_0$ and $p_{1,2}$ are the eigenvalues of Eq. (6) for $\sigma = -1$. Application of this solution and matching boundary conditions at the barrier points $q_{1,2}$ gives the relaxation oscillation periods in terms of the current and the system parameters. The eigenvalue p_1 is relatively large compared to p_2: $p_1 \approx k'$, $p_2 \approx \frac{1}{k'}$. The result is the following asymptotic expressions for the relaxation oscillation period $T(I')$ and amplitudes in terms of the system control parameters

$$T(I') \to k' \ln \left[\frac{(2q_2 - q_1 - I')(I' + q_2 - 2q_1)}{(q_2 - I')(I' - q_1)} \right], \;\; \text{where} \;\; k' = \frac{3}{4\sqrt{b}}(q_1 - q_2)^2 \qquad (7)$$

$$V_{\max} = 2q_2 - q_1, \;\; V_{\min} = 2q_1 - q_2 \;\; \text{if} \;\; q_1 < I' < q_2, \quad \text{and} \;\; \infty \;\; \text{otherwise} \qquad (7')$$

$$\Big[q_1 < I' < q_2 \Big] \;\; \text{and} \;\; [T \to \infty, V \to 0, \;\; \text{otherwise}] \; .$$

where $q_{1,2}$ are from Eq. (2) and k' follows from $k = \frac{3}{\sqrt{b}}$ and its definition in Eq. (6). Derivation of this result is given in the Appendix. This expression for the period demonstrates logarithmic approach to steady state behavior as I' approaches the barriers $I'_{1,2} = q_{1,2}$ $[T \to \infty]$. Furthermore, the period is a minimum at $I_{\min} = \frac{q_1 + q_2}{2}$, at which point $T_{\min} = T(I_{\min} = 2k' \ln 3$ which is identical to the asymptotic period of the symmetric Stoker-Haag oscillator [Stoker, 1950; Phillipson & Schuster, 2001].

5 Discussion: A Spiking Model

The F-N model of Eq. (1) is a particular example of two dimensional dynamical systems $\frac{dV}{d\tau} = F(V,Y)$, $\frac{dY}{d\tau} = G(V,Y)$ that facilitates the construction of nullclines and phase plane analysis which are powerful tools for the analysis of bifurcation and oscillation phenomena [Murray, 1989; Izhikevich, 2000]. The present approach considers dynamical mechanisms expressed as N coupled first order nonlinear differential reformulated as one $N-$th order nonlinear differential equation. The passage to Eq. (2) is an example for $N = 2$, The analysis of Nagumo *et. al* of neuron conduction is an example for $N = 3$ as well as later bifurcation studies of some canonical three dimensional systems [Phillipson & Schuster, 2000]. For the present example, the consequent Reduced Model of Eq. (3), preserving to close approximation the pulse dynamics and of the F-N model, facilitated approximate analytical determination of the period and extrema of the pulses in terms of the physiological parameters $[a, b, \epsilon]$ of the system. The subsequent Reduced Broken-Linear Model allows for exact solution with a qualitative change in the pulse shape from convex to concave. The former is more in accord with the H-H model, yet it is of interest to note that the latter is demonstrated under certain parameter conditions by the Morris-Lecar model [Morris & Lecar, 1981]. The three physiological parameters, upon adjustment, can change the pulse form to a limited extent. In particular reducing the stiffness constant can produce almost harmonic oscillations also demonstrated by the Morris-Lecar model.

The Reduced Broken-Linear Model by having explicit solution Eq. (6) provides an analytic mechanism spiking model. The pulses would be observationally characterized by their height $[V_{\max}]$, depth $[V_{\min}]$, and period T. The spiking model is posited to be exactly Eq. (3) according to $q_1 = \frac{V_{\max}+2V_{\min}}{3}$, $q_2 = \frac{V_{\min}+2V_{\max}}{3}$ from Eq. (7') and the spike periods given by Eq. (7). An example of such a spike is the red pulse in Fig. 2. In principle, these observational quantities are related to the physiological parameters $[a, \epsilon]$ by $q_{1,2}$ defined in Eq. (2). The period of the pulse is asymptotically proportional to the stiffness constant which is a sensitive function of b according to $b^{\frac{1}{2}} = \frac{3(q_1-q_2)^2}{4k'}$. A spike occurs whenever the action potential crosses the threshold at q_1 and recrosses it again after period T of Eq. (7) without resetting the action potential characteristic of the Integrate and Fire model (which can be related by transformation to the spiking displayed by the canonical Class I model) [Gerstner & Kistler, 2002]. If one considers more general synaptic inputs produced by the current most generally being a function of time, the driving terms in Eqs. (2,3,4) include both $I(\tau)$ and $\frac{dI}{d\tau}$ for which analytic solutions for arbitrary I can be simply arrived out for the Reduced-Broken Linear Model. In particular, a periodic $I(\tau)$ can produce multiple periodicity, bistability, entrainment and chaos for the same dynamical reasons that they arise in the harmonically forced van der Pol equation or its Broken-Linear reduction of the harmonically driven

Stoker-Haag equation [Phillipson & Schuster, 2001]. Linearization of the F-N equations around fixed points in its phase plane representation with an imposed time dependent input has demonstrated some of these phenomena [Di Garbo et al., 2001]. In the present formulation, which will be explored, Eq. (4) represents an alternative dynamical description which by construction is global.

Acknowledgements

Financial support of this work through a visiting professorship from the Austrian Academy of Sciences and support from the University of Colorado at Boulder to one of us (P.E.P) is gratefully acknowledged.

References

Cole, K. S., Antosiewicz, H. A., & Rabinowitz, P. [1955]. "Automatic computation of nerve excitation". *J. Soc. Indust. Appl. Math.* **3**, 153–171.

Cooley, J. W. & Dodge, Jr., F. A. [1966]. "Digital computer solutions for excitation and propagation of the nerve impulse". *Biophys. J.* **6**, 583–599.

Di Garbo, A., Barbi, M., & Chillemi, S. [2001]. "Dynamical behavior of the linearized version of the FitzHugh-Nagumo neural model". *Int. J. Bifurcation and Chaos* **11**, 2549–2558.

Dorodnitsyn, A. A. [1947]. "Asymptotic solution of van der Pol's equation". *Priklad Mat. I. Mekh.* **11**, 313–328. In Russian. English translation: *Trans. Am. Math. Soc.* **88** [1953], 1-24.

FitzHugh, R. [1961]. "Impulses and physiological states in theoretical models of nerve membrane". *Biophys. J.* **1**, 445–466.

FitzHugh, R. & Antosiewicz, H. A. [1959]. "Automatic computation of nerve excitation – detailed corrections and additions". *J. Soc. Indust. Appl. Math.* **7**, 447–458.

Gerstner, W. & Kistler, W. [2002]. *Spiking Neuron Models*. Cambridge University Press. New York.

Hodgkin, A. L. & Huxley, A. F. [1952]. "A quantitative description of membrane potential and its application to conduction and excitation in nerve". *J. Physiol.* **117**, 500–544.

Izhikevich, E. M. [2000]. "Neural excitability, spiking, and bursting". *Int. J. of Bifurcation and Chaos* **10**, 1171–1266.

Jackson, E. A. [1991]. *Perspectives of Nonlinear Dynamics*. Volume 1 and 2. Cambridge University Press. Cambridge, UK.

Krylov, N. & Bogoliubov, N. [1947]. *Introduction to Non-Linear Mathematics*. Priceton University Press. Princeton, NJ.

Mascagni, V. S. & Sherman, A. S. [1998]. "Numerical methods for neuronal modelling". In Koch, C. & Segev, I., editors: *Methods in Neuronal Modeling*. Pages 569–606. MIT Press. Cambridge, MA.

Morris, C. & Lecar, H. [1981]. "Voltage oscillations in the barnacle giant muscle fiber". *Biophys. J.* **35**, 193–213.

Murray, J. D. [1989]. *Mathematical Biology*. Springer Verlag. New York.

Nagumo, J., Arimoto, S., & Yoshizawa, S. [1962]. "An active pulse transmission line simulating axon". *Proc. IRE* **50**, 2061–2071.

Phillipson, P. E. & Schuster, P. [2000]. "Bifurcation dynamics of three-dimensional systems". *Int. J. of Bifurcation and Chaos* **10**, 1787–1804.

Phillipson, P. E. & Schuster, P. [2001]. "Dynamics of relaxation oscillations". *Int. J. of Bifurcation and Chaos* **11**, 1471–1482.

Rinzel, J. [1978]. "On repetitive activity in nerve". *FASEB Proc.* **37**, 2793–2802.

Rinzel, J. [1981]. "Models in neurobiology". In Enns, R. H., Jones, B. L.,

Miura, R. M., & Rangnekar, S. S., editors: *Nonlinear Phenomena in Physics and Biology*. Pages 345–367. Plenum Press. New York.

Rinzel, J. & Ermentrout, G. B. [1998]. "Analysis of neural excitability and oscillations". In Koch, C. & Segev, I., editors: *Methods in Neuronal Modeling*. Pages 251–291. MIT Press. Cambridge, MA.

Scott, A. C. [1975]. "The electrophysics of a nerve fiber". *Rev. Mod. Phys.* **47**, 487–533.

Stoker, J. J. [1950]. *Nonlinear Vibrations in Mechanical and Electrical Systems*. Interscience Publishers. New York.

Troy, W. C. [1976]. "Bifurcation phenomena in FitzHugh's nerve conduction equations". *J. Math. Anal. & Appl.* **54**, 678–690.

Appendix: Calculation of the period in Eq. (7)

Figure 3 shows a representative closeup solution [$I = 0.3$] of the Reduced Broken-Linear Model, Eq. (4) for $V(\tau)$ (black curve) and $v(\tau) \equiv \frac{dV}{d\tau} = \frac{dx}{d\tau}$ (red curve). Following a procedure identical to that applied to calculation of the period for the symmetric oscillations of the Stoker-Haag oscillator [Phillipson & Schuster, 2001] we consider the system initially at point **a** at the lower boundary: $V_0 = q_1 = I' + x_0,\ \ v(0) = v_{s1}$ and arriving at point **b** at some time T_1 such that $V(T_1) = q_2 = I' + x(T_1), v(T_1) = v_{f1}$ where from the velocity curve it is seen that $v_{s1} << v_{f1}$. Then from Eq. (6) for $\sigma = -1$

$$x(T_1) = q_2 - I' = \frac{v_{s1} - p_2(q_1 - I')}{p_1 - p_2} \exp(p_1 T_1) + \frac{p_1(q_1 - I') - v_{s1}}{p_1 - p_2} \exp(p_2 T_1) \tag{A.1}$$

$$v(T_1) = v_{f1} = \frac{p_1\Big[v_{s1} - p_2(q_1 - I')\Big]}{p_1 - p_2} \exp(p_1 T_1) + \frac{p_2\Big[p_1(q_1 - I') - v_{s1}\Big]}{p_1 - p_2} \exp(p_2 T_1) \tag{A.2}$$

so that

$$\exp(p_1 T_1) = \frac{(p_1 - p_2)(q_2 - I') - \Big[p_1(q_1 - I') - v_{s1}\Big] \exp(p_2 T_1)}{\Big[v_{s1} - p_2(q_1 - I')\Big]} \tag{A.3}$$

$$v_{f1} = p_1[q_2 - I'] + \Big[v_{s1} - p_1(q_1 - I')\Big] \exp(p_2 T_1)\ . \tag{A.4}$$

Since $p_1 p_2 = 1$, from Eq. (A.3), $T_1 \approx p_2 \approx \frac{1}{k'} \to 0$ and to the same approximation $v_{s1} \to 0$ [Phillipson & Schuster, 2001] so that Eq. (A.4) establishes v_{f1} according to

$$v_{f1} \approx p_1(q_2 - q_1) \to k'(q_2 - q_1)\ . \tag{A.5}$$

From point **b** the system evolves through an oscillation maximum and then back to the upper barrier in the asymptotically longer time T_2 such that at point **c** $V(T_2) = q_2 = I' + x(T_2),\ \ v(T_2) = v_{s2}$. Then from Eq. (6) for $\sigma = +1$, with $\exp -p_1 T_2 \approx \exp -(k' T_2) \to 0$

$$x(T_2) = q_2 - I' = \frac{v_{f1} + p_1(q_2 - I')}{p_1 - p_2} \exp(-p_2 T_2) \to \Big[\frac{v_{f1}}{k'} + q_2 - I'\Big] \exp(-\frac{T_2}{k'}) \tag{A.6}$$

so that with the use of Eq. (A.5)

$$T_2 \to k' \ln \frac{\Big[2q_2 - q_1 - I'\Big]}{q_2 - I'} \tag{A.7}$$

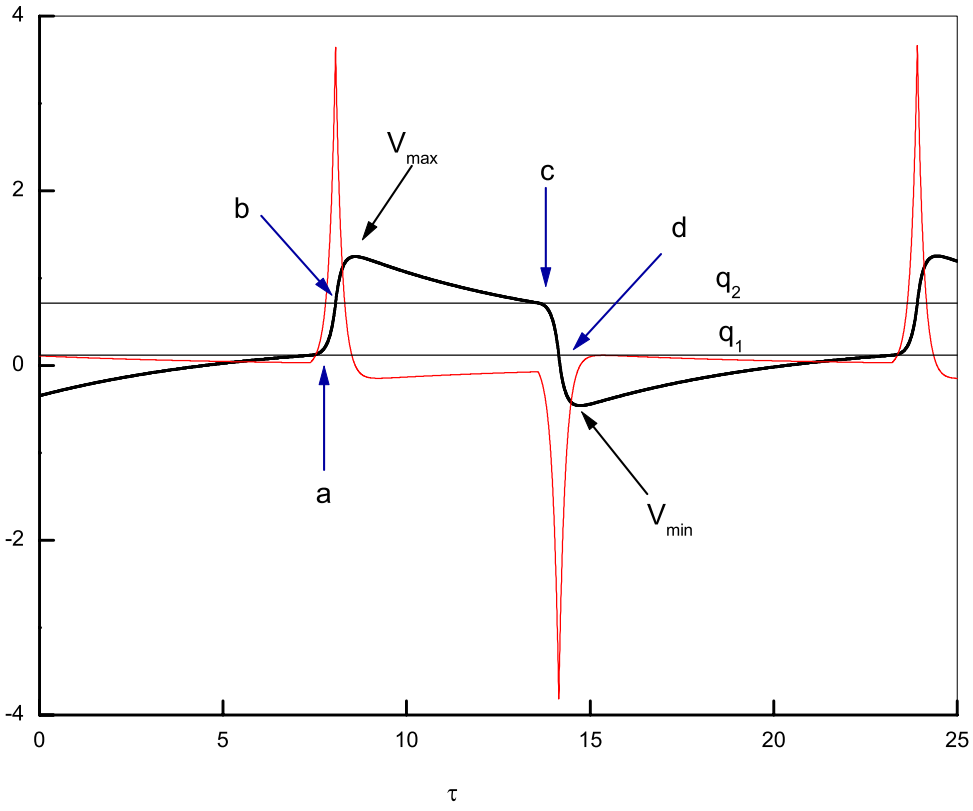

Fig. 3. **Close-up of a typical relaxation oscillation of the Reduced Broken-Linear Model, Eq. (4) with $I = 0.3$.** Shown are the potential $V(\tau)$ (black curve) and the velocity $v \equiv dV(t)/dt$ (red curve). This figure illustrates the elements for the period and pulse maximum, minimum of Eqs. (7,7') as derived in the Appendix. The system points shown are**a**: $V = q_1$, $v = v_{s1}$; **b**: $V = q_2$, $v = v_{f1}$; **c**: $V = q_2$, $v = v_{s2}$; **d**: $V = q_1$, $v = v_{f2}$. The analytic expressions for the pulse period are in the asymptotic approximation that $v_{s1,2} \approx \frac{1}{k'} \to 0$, $v_{f1,f2} \approx k' >> 1$. This is tantamount to neglecting the transition times between the barriers compared to the time spent above and below the barriers.

From point **c** the system point again enters the inter barrier region at $V_0 = q_2$ with the asymptotically small speed v_{s2} and making again a fast transition in time T_3 to the lower barrier such that $x(T_3) = q_1 - I'$, $v(T_3) = v_{f2}$. From Eq. (6), again with $\sigma = -1$ with the same approximations used in traversing **a** to **b**, one obtains $v_{s2}, T_3 \to 0$ and $v_{f2} \to -p_1(q_2 - q_1) = -v_{f1}$. The oscillation is completed when the system makes its final excursion from point **d** to the beginning point **a** in long time T_4 such that $x(T_4) = q_1 - I'$, $v(T_4) = v_{s1} \to 0$. From Eq. (6) with $\sigma = +1$ one obtains, similar to Eq. (A.6) for the path from **b** to **c**

$$\exp(-p_2 T_4) \approx \frac{(p_1 - p_2)(I' - q_1)}{\left[p_1(I' - q_1) - v_{f2}\right]} \tag{A8}$$

so that asymptotically

$$T_4 \to k' \ln \frac{\left[I' + q_2 - 2q_1\right]}{I' - q_1} \tag{A9}$$

The period of oscillation, $T = T_2 + T_4$ using Eqs. (A.7,A.9) gives Eq. (7).

For the pulse maximum we assume a time duration $T_{\max}$ from the time the system point makes a fast transition from point **b** $[x(0) = q_2 - I',\ v(0) = v_{f1}]$ to the pulse maximum $V_{\max}$. Similarly, there is a time duration $T_{\min}$ for the system point to make a fast transition from point **d** $[x(0) = q_1 - I',\ v(0) = v_{f2} = -v_{f1}]$ to the pulse minimum $V_{\min}$. The solutions during these times are for $\sigma = +1$ and with the use of Eq. (A.5) they are given by

$$V_{\max} \approx I' + \left[\frac{p_1(q_2 - q_1) + p_1(q_2 - I')}{p_1 - p_2}\right] \exp(-p_2 T_{\max}) \tag{A.10}$$

$$V_{\min} \approx I' + \left[\frac{-p_1(q_2 - q_1) + p_1(q_1 - I')}{p_1 - p_2}\right] \exp(-p_2 T_{\min}) \tag{A.11}$$

Calculation of $\frac{dV}{d\tau} = 0$ at time $T' \equiv T_{\max,\min}$ shows that asymptotically, $\exp(-p_1 T') \approx p_2^2 \to 0$ resulting in neglect of this term in the solution of Eq. (6). Similarly, $\exp(-p_2 T') \approx (p_2^2)^{p_2^2} \to 1$. With this result,and neglecting $p_2 \approx \frac{1}{k'} << 1$ compared to $p_1 \approx k' >> 1$ Then the I' terms vanish in Eqs. (A.10,A.11) resulting in Eq. (7') for the pulse maximum and minimum.